Assessment of St. St. 316L joints welded by laser beam and metal active gas MAG processes

IOP Conf. Series: Materials Science and Engineering **973** (2020) 012027 doi:10.1088/1757-899X/973/1/012027

Assessment of St. St. 316L joints welded by laser beam and metal active gas MAGprocesses

AM Magdy[1,3]**, AB El-Shabasy**[2,3] **andHA Hassan**[2,3]
[1] Assistant Lecturer,
[2]Professor
[3]Ain Shams University, Faculty of Eng., Design & Prod. Eng. Dept.
ayman_hussien@eng.asu.edu.eg

AbstractStudy the welding of Stainless steel 316L sheet was carried out using two welding techniques, Laser beam and Metal Active Gas MIG. Strips of 1.5 mm thick were cut from the Stainless-steel sheet and then welded using nitrogen gas for shielding. Metallographic examination using optical microscopy and SEM was conducted to study the microstructure of the welded joints. The tensile stress for joints welded by Laser beam and MAG were ranged from 386 to 632 MPa and from 126.5 to 599 MPa respectively according to the parameters of each welding techniques. The average of microhardness values measured at successive distances for joints welded by Laser beam and MAG were 265 HV and 261 HV, respectively. The obtained results were analysed and discussed based on the recent research.

1.Introduction

Austenitic stainless steels are a group of the materials that have the highest service performance in industry, besides their high weldability percent and economical nature. They have a high corrosion resistance due to the high chromium percentage that ranges from 16 to 26% and the presence of Nickel that reaches 20%[1]. 316L grade is one of the most common types that is characterized by its high immunity from sensitization, pitting and crevice corrosions resistance in warm chloride environments, and to stress corrosion cracking above 60 ^{o}C. It has a good oxidation resistance up to about 900 ^{o}C in continuous work.

Na Zhang Liu and Walcott [2] made a series of experiments to investigate correlations between welding parameters and the weld pool geometry. He found a significant nonlinearity in the diode laser welding process and it was found the model takes the reciprocal of the welding speed as the input and the top side surface width of the weld pool as the output.Seang, David and Ragneau[3] studied the effect of Nd:YAG laser welding parameters on the hardness of lap joint. They observed the interaction between the welding parameters and it was reported that the hardness along the depth of the weld bead is affected strongly by the parameters, but they have no influence on the hardness inside the softening zone. Wang et. al. [4] investigated the ductility of laser welded joint by applying three-point bending test. It was clear from their experiments thatthe decrease of heat input by the laser beam welding will increase the ductility of the welded joint. The presence of fine and irregular grains leads to better crack propagation resistance and higher fracture strains.

Sun et. al. [5] showed various advantages such as HAZ was narrow and the grain growth degree was small. Moreover, it could well satisfy motor vehicle exhaust pipe production.Khan et. al.[6]stated that the weld penetration and width mainly increase at higher laser power values because this leads to higher energy deposition on the weld area and the deposited energy will have longer time to diffuse in

the material.Xueet. al.[7]reported that high penetration rate can be achieved when the range of laser power reached 60% and full penetration at laser power greater than 60%. However, microstructure showed that penetration depth is directly proportional with the welding speed. They explained that the temperature of the material increased with increasing welding speed while the cooling time decreased, hence the ability of the laser beam to penetrate the material is increased at higher welding speeds. El-Batahgyet. al. [8] showed that low welding speeds increased the fusion zone dimensions incredibly rather than higher speeds. El-Batahgy[9], Y.Feng et. al. [10] concluded that welding speed had an opposite effect on the penetration depth and bead width, when welding dissimilar joint of austenitic stainless steel joint.Bolut Kong et. al. [11] reported after their trials to weld 6 mm thick stainless steel by Yb-fibre continuous wave laser that full penetration is achieved below 4m/min when the laser power is 5kW, and 1 to 2 m/ min when the laser power is greater or equal to 4kW, and 0.5 m/ min at minimum power of 2.5kW.

Mitsuhiro Okayasu et. al. [12] confirmed that the tensile strength of the welded samples were higher than the base metal when he welded commercial cold rolled low carbon steel by MIG welding. It was also observed that the endurance limit of some samples is higher than the base metal and any other sample.Sin Lin et. al. [13] studied the mechanical properties of MIG welded samples from extruded Al-Mg-Si and it was observed that the ultimate tensile strength of the welded metal is 76.5% from the base metal and the fracture appeared at the least hardened location in the HAZ. The microstructure examination showed the presence of equiaxed coarser grains in the centre zone of the welded samples than the top and side zones.Sudhir Kumar et. al. [14] investigated the effect of preheating, current and voltage on welded steel joint by MIG. The results showed that the efficiency of the joint reached 94.37% at 275 ^{o}C preheating temperature, 120 Ampere, and 35volt. It is also confirmed that the ultimate strength and percent elongation are affected greatly by preheating temperature and the current.

2.Experimental Procedure

Stainless steel sheets of 1.5mm thickness were cut to 30mm width and 200 mm length by wire EDM to obtain high precise cuts. MAG electrode wire of 1 mm was chosen for this experiment.The chemical compositionof the used stainless steel sheets used in this work and the welding wire electrodeobtained from spectroscopy analyser isshown in table 1 and table 2 respectively. The stainless steel sheet is specified according to ASTM A240-12 and the welding electrode is typical to the specifications of AWS 5.9.

Table 1. Chemical composition of 316L stainless steel sheet.

C	Mn	P	S	Si	Cr	Ni	Mo	N
0.03	0.97	0.072	0.006	0.49	16.86	9.73	2.0	0.1

Table 2. Chemical composition of MIG Welding electrode**.**

C	Mn	P	S	Si	Cr	Ni	Mo	N
0.02	1.73	0.032	0.37	0.37	18.87	12.37	2.3	0.13

Figure 1 shows the laser welding robotic arm used in this work. It is a solid-state Nd: YAG laser pump with maximum power of 2.2kW and focal point of 500 µm, which used for welding processes. The laser beam is delivered through a fibre optic cable which is connected to the focusing lens that is fixed in a robotic arm

Figure 1. Laser Welding robotic arm.

MAG weldingWas carried out by using a designed CNC 3 axis machine and Gedik welding machine of Maximum current of 600 Amp as shown in figure 2.

The specimens are cleaned with ethyl alcohol to remove any impurities that may affect the weld bead properties and are held in a custom fixture designed for the experiment and fixed by toggle clamps as shown in figure 3 to prevent the distortion of welded samples by residual stresses. The gap between 2 parts are adjusted to be zero.The ranges of Laser and MIG welding parameters were selected and arranged by designing a factorial experiment as shown in table 3 andtable 4. Two replications were added in the factorial experiments of both MIG and Laser welding. The number of samples of laser were 18 and the number of samples of MIG were 54.Nitrogen is used as shield gas. The flow rate of the shield gas was kept constant at 30 l/min during the whole experiment.

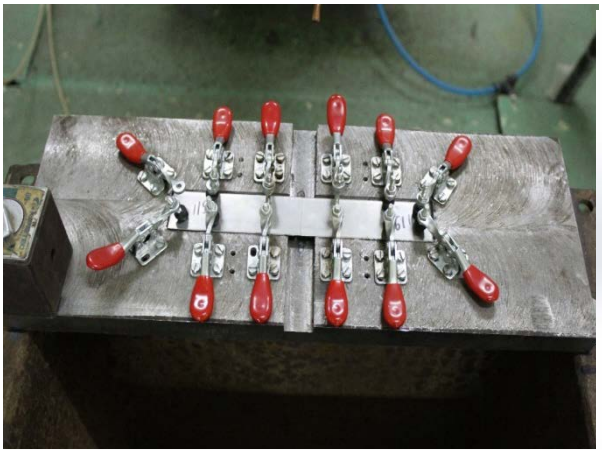

Figure 2. Specimen fixture used during welding processes

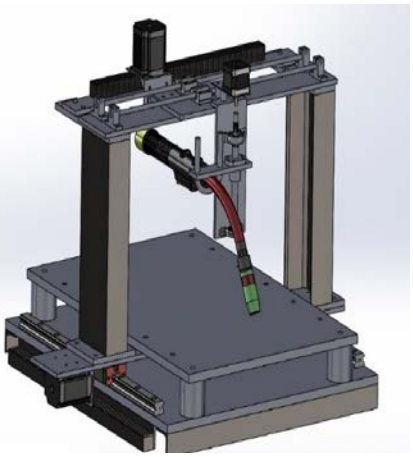

Figure 3. MAG welding CNC

Table 3. Laser Welding parameters ranges**.**

Laser Power (W)	Welding Speed (m/min)
800	0.5
1000	1
1200	1.5

Table 4.MAG welding parameters ranges**.**

Current (Amp)	Welding Speed (m/min)	Wire Feed (rpm)
50	0.5	25
60	1	35
70	1.5	60

The values of the laser power and speed are programmed in the machine. The track is positioned such that the weld line is straight. The height is adjusted to achievezero focal point and in the middle weld line to equally distribute the power density and to prevent any probability offormation of amisaligned welded joint.
The MIG power and wire feed speed were adjusted in the MIG head and the welding speed, weld position and torch height were adjusted in the CNC controller.

To make sure that the welding process is stable, the process is started and ended 5 mm away from the samples. After the end of the welding process, the sample is kept for a short period to cool down and then the clamps are released to fix another sample. Visual inspection was carried out on all the welded sheet to ensure the welding quality. Then the defect free welded joints were subjected to next step of specimen's preparation for the further tests and examination.

EDM wire cut method has been used to get high precision dimensions' specimens used for the mechanical testing as well as macroscopic and microscopic examination. The tension samples were cut according to ASTM E8M-04 standard as shown in figure 4 .The strain rate of the test was adjusted at 4.5 mm/min.

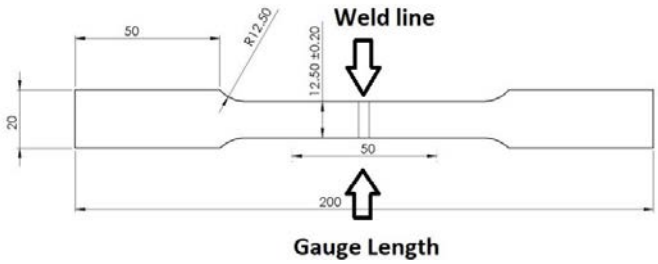

Figure 4. Tensile test specimen standard.

Moreover, other samples were cut and prepared for macroscopic examination of the weld bead. The samples were electro etched by 10% oxalic acid to reveal the welded zone of the sample. Analysis has been performed using metallographic macroscope with image analysis software.
Microhardness test is applied at 100 gram-force and dwell time 20 seconds and the distance between each indentation is adjusted to be 100 µm.
Tensile specimens fracture surfaces have been examined using SEM to reveal the failure type and feature of the fracture surfaces.

3.Results and discussion

3.1 Visual Inspection
The Visual inspection of the Laser showed no sign of imperfections or any air voids as shown in figure5 and this is a prove of thermal stability of laser during the operation.on the other hand,the inspection ofMAG welding specimens has shown some imperfections in some samples and this means that some parameters values did not provide stable heat input during welding. The results are shown in figure 6.

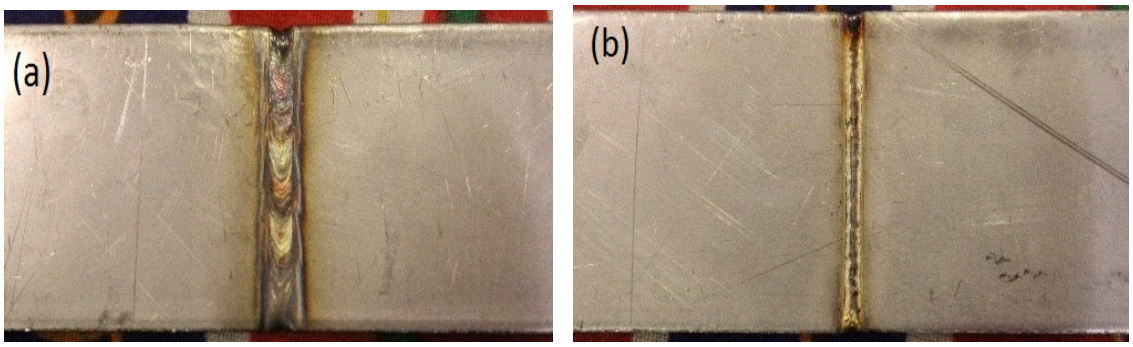

Figure 5. Laser welded specimens at (a) 1000 W, 0.5 m/min. (b) 1000 W, 1 m/min

Figure 6. Discontinuities in MIG welded samples at (a) 70 Amp, 0.5 m/min, 60 rpm. (b) 50 Amp, 0.5 m/min, 35 rpm.

3.2.Mechanical properties

Table 5shows that the Average ultimate stress and max strain of laser welded samples of 12 samples.It is noted that the stress increases with increasing laser power at the same speed and that the stress decreases at an increase in the speed. Due to the small surface area subjected to the load, the material was fractured at the weld area. Tension test was applied on 26 accepted samples and the average results of tension test forMAG specimensare shown in table 6. It is noted that the ultimate tensile strength increases by the increase of MAG welding current and decreases by the increase of welding speed or wire feed rate. In addition, the welding speed and wire feed rate are mutual to each other, such that the change of one of them without the change of the other will affect the quality of the weld, which are illustrated in figures 7 and 8.

Table 5.Average maximum stress at different welding power and speed values.

Power (W)	Welding speed (m/min)	Ultimate Strength (MPa)	Elongation %
800	0.5	580.53	1.58
1000	0.5	631.85	2.55
1000	1	385.77	1.72
1200	0.5	605.21	3.92
1200	1	474.09	2.18
1200	1.5	521.52	1.23

Table 6.Average MAG tension test resultsat different welding parameters.

Current	Welding Speed (m/min)	Wire Feed (rpm)	Ultimate Strength (MPa)	Elongation %
60	0.5	25	368.7	14.1
70	0.5	25	445	34.5
60	0.5	35	508.7	30.5
70	0.5	35	597.65	72.5
60	1	25	456.6	3.7
70	1	25	521.65	47
50	1	35	260.15	4.7
60	1	35	298.6	9.2
70	1	35	480.4	30.3
70	1	60	387.8	17.9
60	1.5	35	126.4	1.4
70	1.5	35	369.3	11.4
60	1.5	60	306.1	6.8
70	1.5	60	303.5	5.9

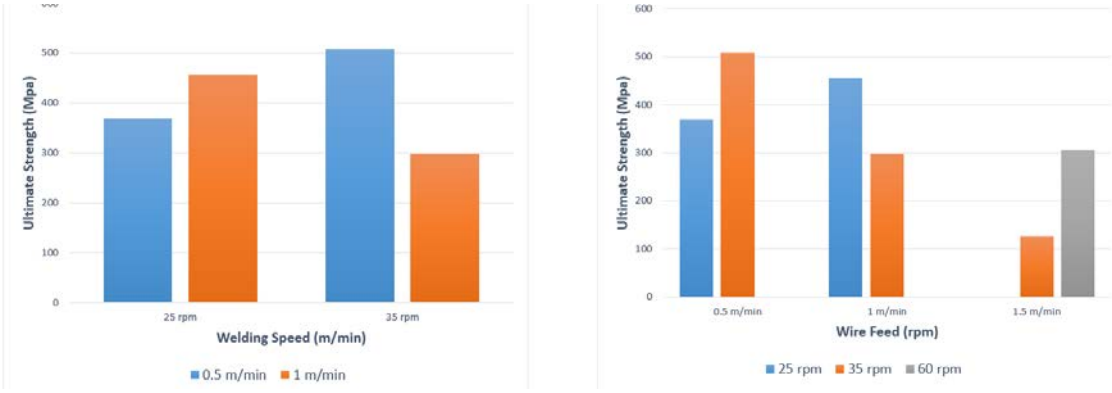

Figure 7. The influence of welding speed and wire feed rate at 60 amp

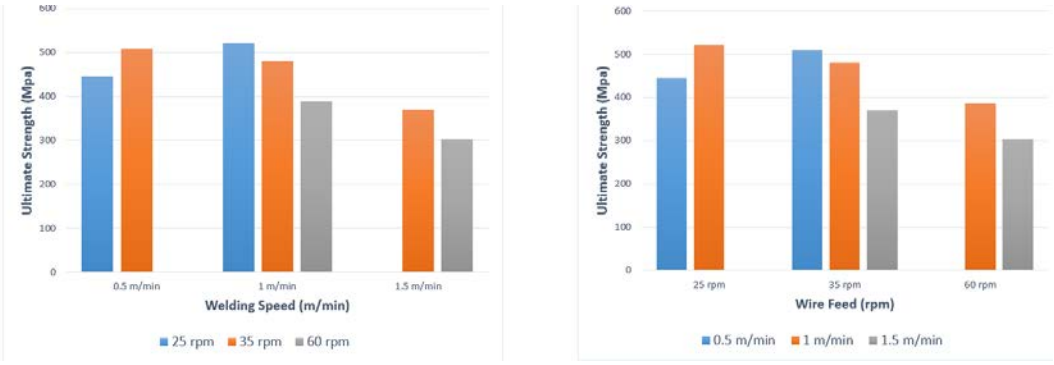

Figure 8. The influence of welding speed and wire feed rate at 70 amp

The Laser welding joints and MAG welding joints fractured surfaces from specimens tested under tension test have undergone SEM examination. The analysis has proved ductile fracture for both techniques and the results are shown figure9 and figure 10, respectively.

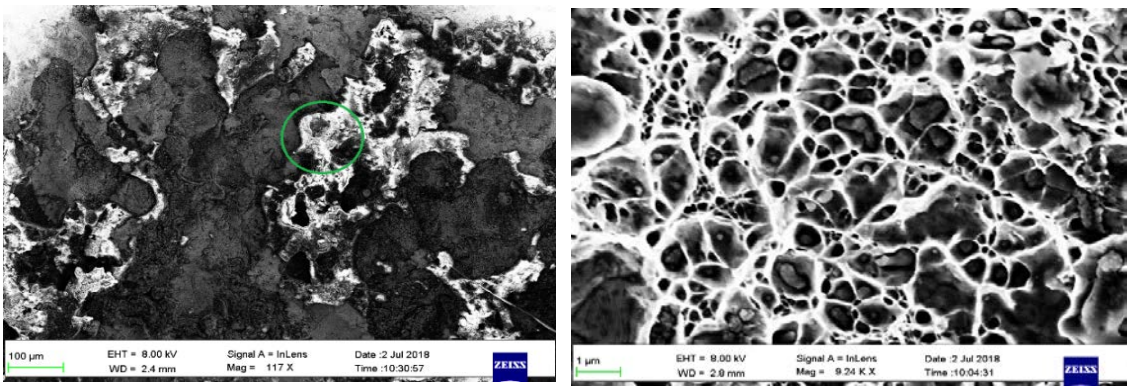

Figure 9. Fracture surface of Laser welded joint at 1200 W, 0.5 m/min using SEM.

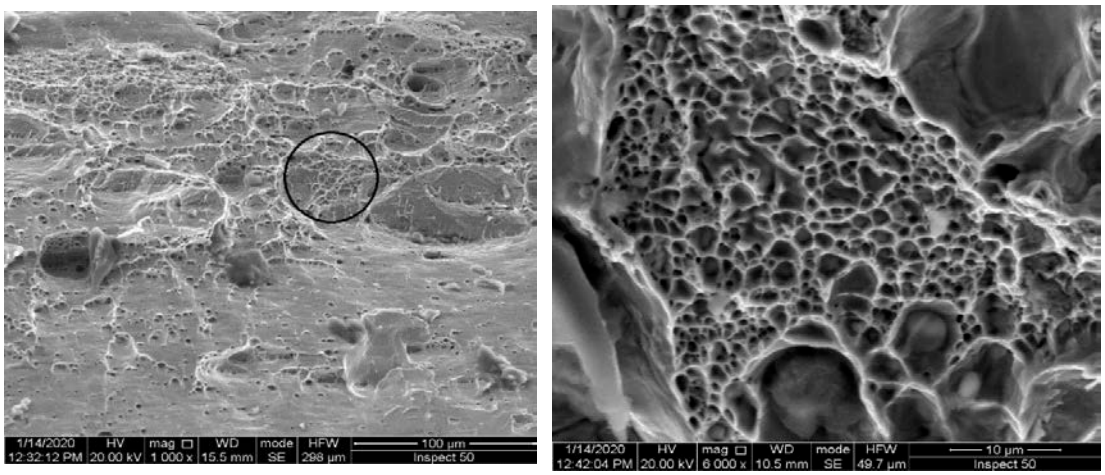

Figure 10. Fracture surface of MAG welded joint at 60-amp, 1 m/min, 25 rpm using SEM.

3.3 Microstructure Analysis

The microstructure of the weld is the main impact in controlling the mechanical properties and service efficiency of the joint. The percentage of the elements in the material and the cooling rate are domaining the nature of solidification and solid-state transformation that dominate the microstructure of the fusion zone. The mode of solidification determines the microstructure shape of the welded zone. EDX analysis was conducted at the middle of the weld zone. The chemical composition of the welded joint is measured by EDX analysis as shown in presented inTable 7, and table8.

According to D.J.Kotecki and T.A.Siewert[15] the equations of $Cr_{eq}$and Ni_{eq} are

Cr_{eq} = %Cr + %Mo + 0.7 %Nb

Ni_{eq} = Ni + 35 %C + 20 %N + 0.25 %Cu

Bsy substituting values in the equations of Creq and Nieq, the results of Laser will be:

Cr_{eq}= 17.97 %

Ni_{eq}= 10.68 %

While the results of MAG will be:

Cr_{eq}=20.49%

Ni_{eq}= 8.65 %

Table 7. EDX Analysis of Laser welded samples.

N	Si	Cr	Mn	Ni	Mo
0	0.317	15.46	0.25	10.68	1.58

Table 8. EDX Analysis of MAG welded samples.

N	Si	Cr	Mn	Ni	Mo
0	0.15	18.12	0	8.65	2.37

TheCr_{eq}/Ni_{eq}ratio of Laser is 1.68, while that of MAG is 2.36. From the pseudo-binary phase diagram (figure 11), the solidification mode of laser is expected to be at Ferrite-Austenite(FA) zone, and the expected ferrite number is 6.8, which indicates that the weld will contain about 6.8% ferrite phase. While the ferrite number for MAG is 18, hence the expected solidification mode of MAG is at Ferrite (F) zone.

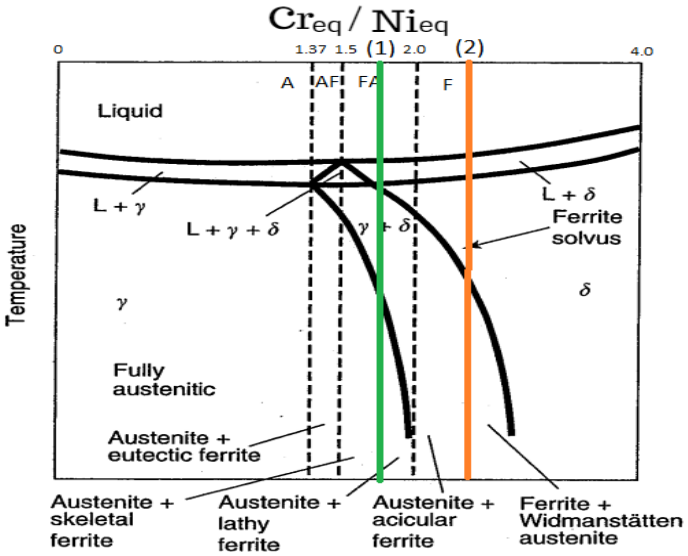

Figure 11. Predicted Solidification mode of (1) Laser, (2) MIG.

The microstructure of Laser welded joint showed different results from expected calculations. With the aid of J.C.Lippold[16],vermicular ferrite was observed which refers to Austenite Ferrite(AF)solidification mode as shown in figure 12(a).It is also observed the presence of skeletal and lathy ferrite phases with some regions of Widmanstatten austenite and intercellular austenite which confirms the primary FAsolidification mode as shown infigure 12(b)

MAG welded joint microstructure showed coarse grains of skeletal ferrite in most regions of the weld, which confirms the occurrence of F solidification mode as predicted in pseudo-binary phase diagramand this is shown in figure 13. The MAG specimens also showed the presence of HAZ that contains precipitates of Ferrite at the grain boundaries, while Laser Samples did not show any HAZ and this is shown in the figures 14 (a) and (b).

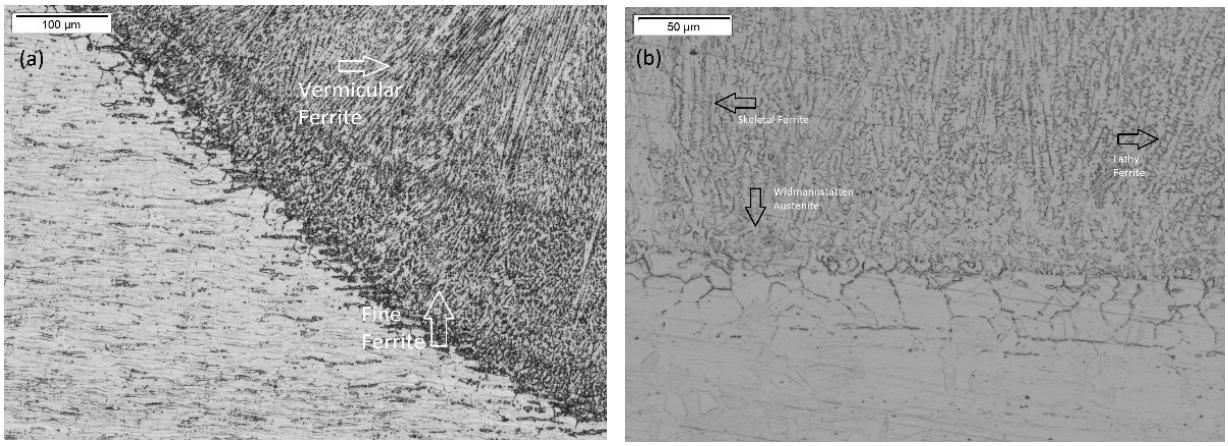

Figure 12. Laser sample microstructure (a) vermicular and fine ferrite microstructure (b)skeletal ferrite, lathy ferrite and Widmannstatten austenite.

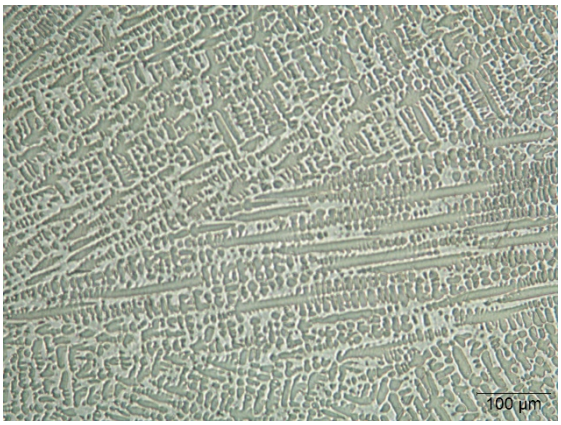

Figure 13. Microstructure of MAG welded joint showing Skeletal Ferrite phase.

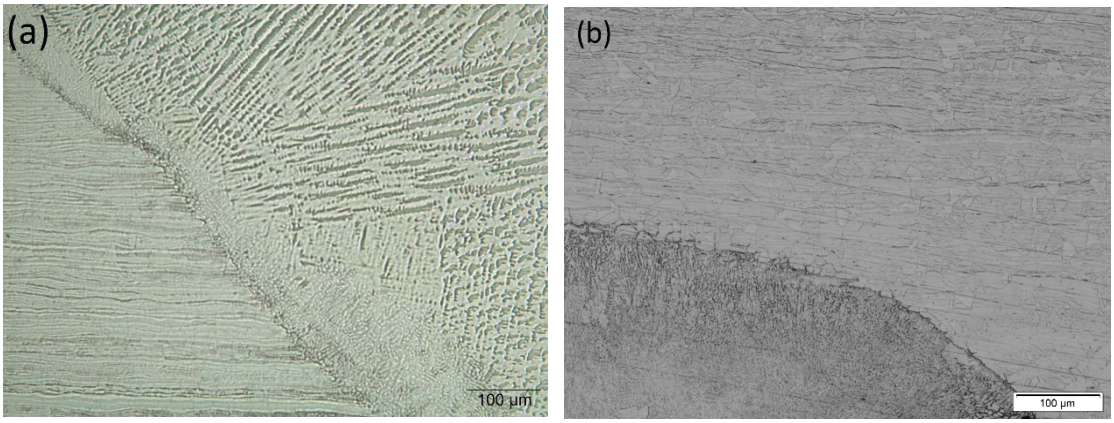

Figure 14. Welded zone boundaries with the base metal in (a) MAG joint and (b) Laser joint

3.4. Microhardness test

Microhardness test is applied on welded specimens to find out whether hardness is the same in different conditions or if there is any change in the hardness value. It is noted that the hardness number of the welds are nearly the same andtheir values are more than that of base metal as shown in figure15andfigure16. The laser weld has non-uniform distribution of material contained in the weld

zone which changes the behaviour of the weld.This leads to a change in the hardness of the material. The appeared peak in the hardness values is due to the presenceof sigma phase in the laser weld bead, which contains 17.42 wt.%of chromium and 2.25 wt.% molybdenum, and this is from the EDX analysis shown in figure 17. While the MAG welded joint has shown that the fluctuations of in the hardness numbers were lower than that of Laser, and this is due to the homogeneity of phase distribution in the major region of the MAG weld bead, hence the change of hardness values is minimised.The average value reported bySeang[3] was 400 HV, while value of 240 HV was achieved by Khan et. al. [17].

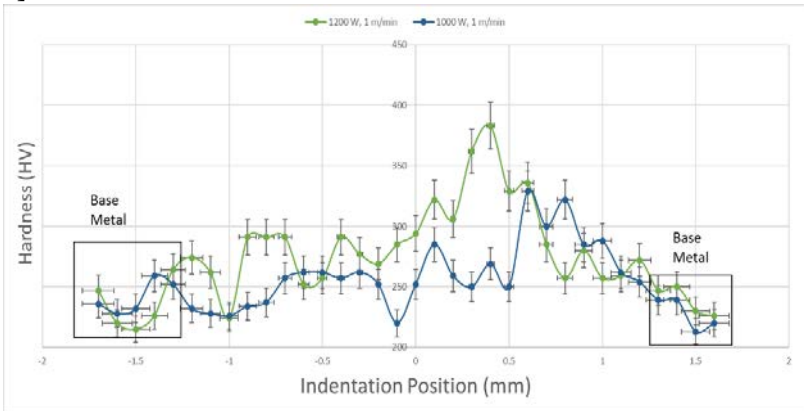

Figure 15. Hardness values across two Laser welded samples at 1200 W and 1 m/min, and 1000 W and 1 m/min.

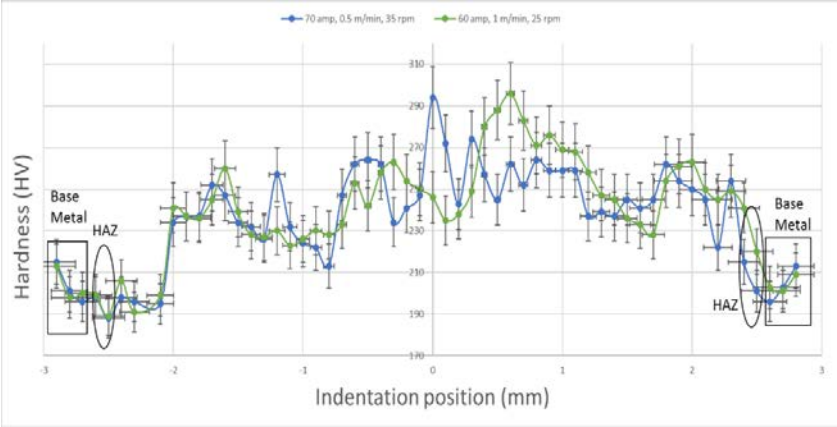

Figure 16. Hardness values of MAG joints at 70-amp, 0.5 m/min, 35 rpm, and 60-amp, 1 m/min, 25 rpm.

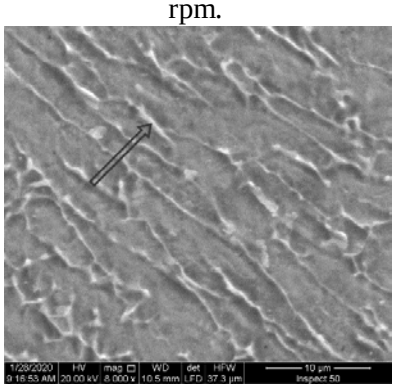

Figure 17.EDX analysis location of sigma phase.

4.Conclusions

Stainless steel 316L sheet has been welded using two welding techniques, Laser beam and Metal Active gas MAG. Based on several results have been obtained from the experimental work, the following conclusions could be drawn:

- The tensile stress for joints welded by Laser beam and MAG were ranged from 386 to 632 MPa and from 126.5 to 599 MPa, respectively.
- The maximum tensile stresses of the Laser specimens were increased by increasing laser power. On the other hand, the increase of the maximum tensile stress values of MAG specimens are independent from increasing current, but they depend on optimising the values of current, welding speed and wire feed.
- The average of Microhardness values measured at successive distances for joints welded by Laser beam and MAG were 265 HV and 261 HV, respectively.
- The microstructure examination revealed that, the laser welded joints have shown dendritic non uniform microstructure which may affect the properties of the microstructure along the weld line. While, the MAG welded joints have shown uniform microstructure, which means that the mechanical properties are distributed equally along the weld line.
- The SEM analysis has shown that the fracture of Laser and MAG welded specimens are ductile, which means that the weld did not have a major effect in the properties of the material.

5.References

[1] Folkhard E 1988 *Welding Metallurgy of Stainless Steels*.
[2] Na X, Zhang Y, Liu Y and Walcott B 2010 *Nonlinear identification of laser welding process* (IEEE Trans. Control System Technology vol. 18 no. 4) pp 927–934.
[3] Seang C, David A K and Ragneau E 2013 *Effect of Nd:YAG laser welding parameters on the hardness of lap joint: Experimental and numerical approach* (Physics Procedia vol 41) pp 38–40.
[4] Wang G, Wu A, Zou G, Zhao Y, Chen Q and Ren J 2009 *Bending Properties and Fracture Behavior of Ti-23Al-17Nb Alloy Laser Beam Welding Joints* (Tsinghua Science and Technology vol. 14 no. 3) p 293–299.
[5] Sun A, Liu J and Liu W 2011 Proc. Int. Conf. Electronic Mechanical Engineering Information Technology EMEIT vol. 8 p 3931–3933.
[6] Khan M M A, Romoli L and Dini G 2013 *Laser beam welding of dissimilar ferritic/martensitic stainless steels in a butt joint configuration* (Opt. Laser Technology vol 49) p 125–136.
[7] Xue X, Pereira A, Amorim J and Liao J 2017 *Effects of Pulsed Nd:YAG Laser Welding Parameters on Penetration and Microstructure Characterization of a DP1000 Steel Butt Joint* (Metals Basel vol 7 no 8) p 292.
[8] El-Batahgy A M, Khourshid A F and Sharef T 2011 *Effect of Laser Beam Welding Parameters on Microstructure and Properties of Duplex Stainless Steel* (Material Science Applications vol 2 no 10) p 1443–1451.
[9] El-Batahgy A M 2012 *Laser Beam Welding of Austenitic Stainless Steels–Similar Butt and Dissimilar Lap Joints* (Welding Processes) p 93–116.
[10] Feng Y, Luo Z, Liu Z, Li Y, Luo Y and Huang Y 2015 *Keyhole gas tungsten arc welding of AISI 316L stainless steel* (Material Design vol 85 no 11) pp. 24–31.
[11] Bolut M, Kong C Y, Blackburn J, Cashell K A and Hobson P R 2016 *Yb-fibre laser welding of 6 mm duplex stainless steel 2205* (Physics Procedia vol 83) pp 417–425.
[12] Okayasu M, Ohkura M, Sakamoto T, Takeuchi S, Ohfuji H and Shiraishi T 2013 *Mechanical properties of SPCC low carbon steel joints prepared by metal inert gas welding* (Material

Science Engineering A vol 560) pp 643–652.
[13] Lin S *et al 2019Microstructures and fatigue behavior of metal-inert-gas-welded joints for extruded Al-Mg-Si alloy* (Material Science Engineering A, vol 745) pp 63–73.
[14] Kumar S and Singh R 2019 *Optimization of process parameters of metal inert gas welding with preheating on AISI 1018 mild steel using grey based Taguchi method* (Measurement vol 148) pp 106924.
[15] Kotecki D J and Siewert T A 1992 *WRC-1992 Constitution Diagram for Stainless Steel Weld Metals□: A Modification of the WRC-1988 Diagram* (AWS Annual Meeting) pp 171–178.
[16] Kotecki D J and John Lippold C 2005 *welding metallurgy and weldability of stainless steels*.
[17] Khan M M A, Romoli L, Fiaschi M, Dini G and Sarri F 2012 *Laser beam welding of dissimilar stainless steels in a fillet joint configuration* (Material Process Technology vol 212 no 4) pp 856–867.